THE PENNSYLVANIA STATE UNIVERSITY
SCHREYER HONORS COLLEGE

DEPARTMENT OF CHEMICAL ENGINEERING

EXPLORING THE EFFECTS OF OVEREXPRESSING AN $NADP^+$-DEPENDENT GAPDH AND THE NAD^+ SALVAGE PATHWAY ON COFACTOR AVAILABILITY FOR NADPH-DEPENDENT BIOTRANSFORMATION IN *ESCHERICHIA COLI.*

RENAE C. PATCH

SPRING 2010

A thesis submitted in partial
fulfillment of the requirements
for a baccalaureate degree in
Chemical Engineering with
honors in Chemical Engineering

Reviewed and approved* by the following:

Patrick C. Cirino
Associate Professor of Chemical Engineering
Thesis Supervisor

Themis Matsoukas
Professor of Chemical Engineering
Honors Adviser

*Signatures are on file in the Schreyer Honors College

ABSTRACT

Improving the efficiency of biocatalytic production of xylitol has been studied by attempting to improve the availability of NADPH, which is a necessary co-substrate in the CbXR-catalyzed reduction of xylose to xylitol in *Escherichia coli* [1]. This research analyzes the impact of coexpressing (along with CbXR) three different enzymes proposed to improve NADPH availability on overall xylitol production, xylitol yield (moles of xylitol produced per mole of glucose consumed, Y_{RPG}). Three novel bicistronic plasmids were constructed in which CbXR is immediately upstream of either *GDP1*, an $NADP^+$-dependent glyceraldehyde-3-phosphate dehydrogenase, *pncB*, encoding nicotinate phosphoribosyltransferase, or *nadK*, encoding nicotinamide adenine dinucleotide kinase.

Xylitol production in the early stages of batch culturing generally showed an increase with the addition of *nadK* or *GDP1* to the system, compared to the expression of only CbXR, while *pncB* caused a decrease in the total concentration of xylitol. Because the standard deviation was so large, the Y_{RPG} values for each enzyme were considered statistically the same as those seen previously with CbXR expression. However, the average Y_{RPG} increased with both *GDP1* and *nadK* while decreasing with *pncB*, and with more data these values may be proven to be statistically significant.

Although the cofactor concentration levels generally increased and decreased as expected according to their associated reactions, the cofactor analysis saw no trends in $NADPH/NADP^+$ ratios when compared to xylitol yields for each enzyme. *GDP1* ratios were much lower, even though the Y_{RPG} increased, and the ratios seen with *pncB* expression were the same as CbXR. The only positive correlation between

NADPH/$NADP^+$ ratios and xylitol yield was seen with *nadK* expression, but the standard deviation on the reported ratios was too large to make any reliable conclusions regarding the specific impact of this enzyme.

TABLE OF CONTENTS

LIST OF FIGURES

LIST OF TABLES

ACKNOWLEDGEMENTS

I would like to personally thank Dr. Patrick Cirino and the entire Cirino lab group for their continued guidance and support throughout the duration of my research experience. As a sophomore with very little background knowledge in field of molecular biology, I had a lot to learn before I could even begin thinking about the research that would eventually become this thesis. Dr. Cirino and all of his lab students were extremely helpful in this regard and never lost hope in my ability to complete this project and come out all the more knowledgeable.

I would especially like to send my gratitude to Jonathan Chin for his endless patience with my questions, poor memory, and busy schedule! He was always available to answer any minor question and even remind me of experiments I should be thinking about while he had his own research and experiments to focus on. Also, Bolaji Akinterinwa often assisted when I was pressed for time, and this was a huge help! Additionally, I owe special thanks to Dr. Peter Richard for providing the p1696 plasmid used for further genetic modification in this project.

Finally, I would like to thank my friends and family for their support of my research endeavor. No matter how many other extracurricular activities I took on, they were encouraging and accommodating of my various time commitments. I appreciate everything they have done for me throughout my Penn State career!

1. INTRODUCTION

The exploration of biocatalysis for production of value-added chemicals is worthwhile for several reasons. Bioproduction provides a safe method considering the less extreme conditions (such as lower temperature and pressure setting) and overall "green" process. Additionally, relatively inexpensive feedstock and enhanced product specificity with bioproduction add to its beneficial characteristics. A specific issue associated with *in vitro* biocatalysis is the high cost associated with continuously delivering the reduced nicotinamide cofactors, NAD(P)H, required for redox reactions within the system [2]. Another drawback lies in the relatively low yield and titer of current biosyntheses. This project addresses both of the mentioned concerns by utilizing whole-cell biocatalysis in *Escherichia coli*.

In vitro studies currently use purified enzymes to couple cofactor regeneration to oxidation of co-substrates such as glucose and formate. For example, formate is chosen due to low cost and catalyzed oxidation to CO_2, which drives the effectively irreversible reaction pair toward greater NADH production seen in Figure 1a. The significance of using formate dehydrogenase (FDH) is that the variation from the "production enzyme" allows specificity for the co-substrate only. A variation of this idea, seen in Figure 1b, is utilized for NADPH production [3].

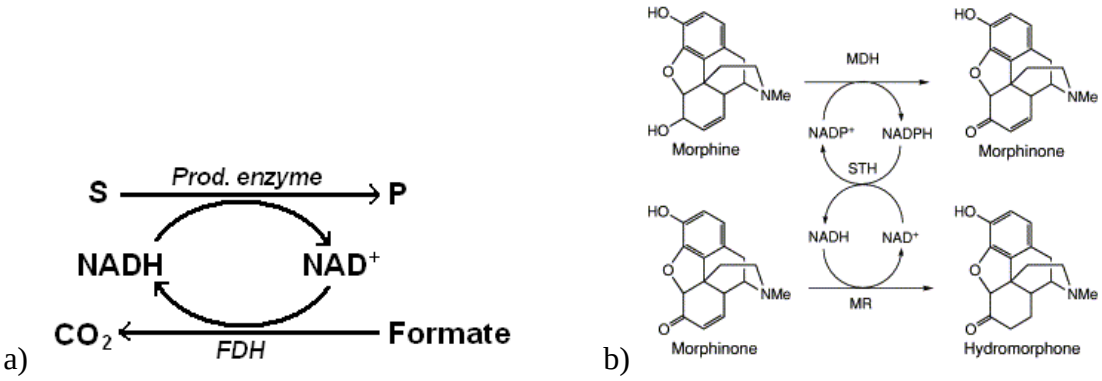

Figure 1: Production of reduced cofactors. (a) Regeneration of NADH from formate oxidation catalyzed by FDH coupled to any reaction relying on NADH. (b) NADPH regeneration using soluble pyridine nucleotide transhydrogenase (STH), morphine dehydrogenase (MDH), and morphinone reductase (MR). Figure (b) taken from Zhao et al. [3]

Whole-cell biocatalysis potentially provides an improved solution to NAD(P)H regeneration. Research groups have studied its advantages over the years [1, 4, 5]. A review by Granstrom et al. discusses the examination of the metabolic pathways as a means to determine where the primary responsibility in supplying NADPH lies [6]. Resources also suggested plasmid-based enzyme overexpression can increase the reduced cofactor pool by making better use of sugar metabolism [1]. For instance, the metabolism of glucose, which reduces $NAD(P)^+$ as a result of overall oxidation to CO_2, produces the required reduced cofactors.

Specifically, this study investigates biosynthetic production of xylitol, a pentahydroxy sugar alcohol, from a feed of xylose and glucose. Small amounts of xylitol can be found naturally in fruits and vegetables, and it is also encountered as an intermediate in mammalian metabolism. Xylitol has a sweetness comparable to that of sucrose, has noncariogenic tendencies (inhibits dental caries), and is unable to reduce the nutritional value of proteins via the Maillard reaction, making xylitol a favorable candidate for

sweeteners, toothpastes, and food additives. Additionally, diabetics benefit from xylitol's non insulin-mediated metabolism. Finally, xylitol acts as a basic starter molecule for other sugars, adding more value to the mass production of this polyol [7, 8].

Several xylitol production methods and technologies have been studied and examined to test their variations in efficiency and feasibility [6]. The quantity of xylitol from natural sources is too small for economical solid-liquid purification. However, industry circumvents this problem by catalytically reducing xylans to produce xylitol. Xylans, which are polysaccharides made of xylose subunits, can be found in birch and beech tree woods, corn stalks, cotton seed, and peanut hulls among other natural sources. While hydrolysis of xylan yields mostly D-xylose (80-85% of total product), it also produces L-arabinose, D-mannose, and D-galactose [9]. Commercially, this hydrolysis is followed by hydrogenation with a nickel catalyst (Ni/Al_2O_3) under high temperature and pressure conditions – up to 140°C and 50 atm – before purification of xylitol [9].

Over the years, interest in microbial production of xylitol has significantly grown [6]. Studies utilizing *Saccharomyces cerevisiae* were first popular, but the spectrum of organisms being engineered to produce xyltiol has expanded to include many *Candida* yeasts. Although there are several organisms known to naturally produce xylitol, we have chosen to work with *E. coli* for several reasons. *E. coli* is a fast-growing organism, requiring relatively cheap growth medium supplements [10]. The genetic manipulation of *E. coli* is simpler than that of yeast strains; gene overexpression, gene deletion, and heterologous gene production can be achieved with standard protocols.

In regards to the efficiency of biosynthetic production of xylitol, Cirino et al. have previously examined various heterologous xylose reductases (XR) and xylulose

dehydrogenases (XDH) and reported that an XR from *C. boidinii* (CbXR) was the most efficient reductase for their *E. coli* system [10]. As seen in Figure 2, XR tends to prefer NADPH over NADH as a substrate, causing the production of this cofactor to become a key limitation in the feasibility of xylitol bioproduction. The idea of NADPH "bottlenecking" bioproduction of xylitol has also been reported by Kötter et al. when using *S. cerevisiae* [11].

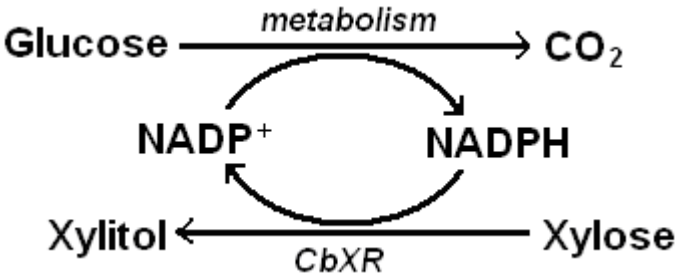

Figure 2: Glucose metabolism coupled with xylose reduction. Note that central metabolism has the ability to reduce either NAD^+ or $NADP^+$, however CbXR typically only uses the converted NADPH.

Since biocatalytic production of xylitol uses xylose as the starting material, the system cannot be allowed to exhibit diauxic growth characteristics by assimilating only glucose preferentially. This being the normal metabolism mechanism, a mutation in the native *crp* gene was developed – binding *crp* to cAMP, thus forming *crp** – to allow for simultaneous glucose and xylose uptake [12]. An alternative method to attain this simultaneous assimilation, which was shown to achieve similar amounts of xylitol produced, requires the plasmid expression of xylose transporters [13].

In this novel system, *E. coli* has the opportunity and ability to metabolize both xylose and glucose. However, the goal is to produce xylitol, requiring most of the xylose fed to be reduced to this form rather than be metabolized by the system. As depicted in

Figure 3, xylose transporters such as *xylFGH* allow the transfer of xylose into the cell. Enzymes interact with intracellular xylose to convert it to either xylitol or xylulose. Additionally, a xylulokinase (*xylB*) furthers the metabolism of xylose by catalyzing the conversion from xylulose to xylulose-5-phosphate, which would then proceed to the pentose phosphate pathway rather than convert back to xylitol. To solve this issue, a strain of *E. coli* was created with the gene encoding xylulokinase removed from the chromosome, also known as the *xylB* knockout (*ΔxylB*). Ultimately, the decision was made not to delete *xylA* because the conversion to xylulose is desired for the case of NADH-dependent xylitol dehydrogenase (XDH)-driven xylitol production [10].

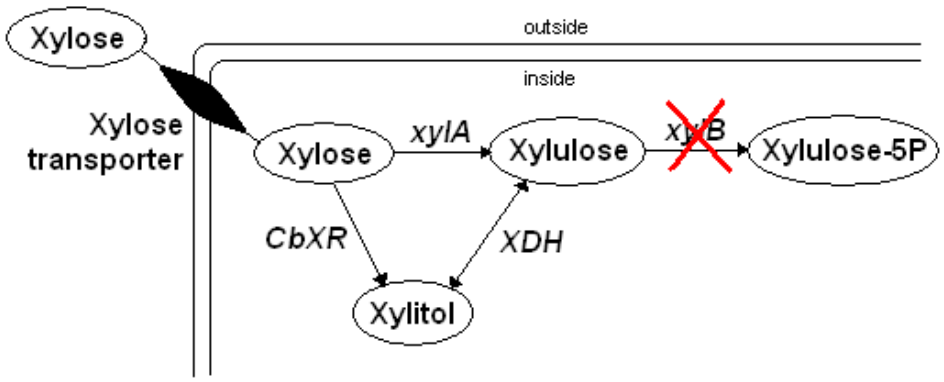

Figure 3: Xylose uptake by cell and metabolism prevention with *ΔxylB*. Note that the xylose transporter role may also be served by a proton symporter known as *xylE*.

The Cirino lab previously demonstrated that in their most efficient xylitol-producing strain, further increases in expression of CbXR or xylose transporters do not result in higher yields. Furthermore, the activity of expressed CbXR was measured (*in vitro*) and determined to exceed the maximum possible rate of reduced cofactor production, given the glucose uptake rates measured during xylitol production (*in vivo*). Ultimately, the

assumption is that the reduced cofactor pool needs to be increased in order to improve xylitol yield (Y_{RPG}) – which has been previously defined as the moles of xylitol product per mole of glucose substrate consumed [1]. The primary focus is on NADPH availability, as it is the cofactor preferred by the reductase in this system, CbXR. This project explores plasmid-based enzyme overexpression to adjust the cofactor pools. The three enzymes examined are an $NADP^+$-dependent glyceraldehyde-3-phosphate dehydrogenase (EC 1.2.1.13, encoded by *GDP1*), nicotinate phosphoribosyltransferase (EC 2.4.2.11, encoded by *pncB*), and nicotinamide adenine dinucleotide kinase (EC 2.7.1.23, encoded by *nadK*)

The transfer of electrons between reduced cofactors is depicted according to the reaction shown in Equation 1. *E. coli* naturally catalyzes this reaction with specific transhydrogenases – in the forward direction with SthA (producing NADH) and the reverse direction with PntAB (producing) NADPH [14].

$$NAD^+ + NADPH \leftrightarrow NADP^+ + NADH \quad (1)$$

GDP1 (1.1 kb) was identified by Verho et al. as an NAD(P)-GAPDH – a gene encoding glyceraldehyde-3-phosphate dehydrogenase that accepts both NAD^+ and $NADP^+$ – in *Kluyveromyces lactis (K. lactis)* [15]. While the characteristic of using $NADP^+$ rather than NAD^+ as cofactor has been observed in plants, this is the only known fungal gene of its kind. As shown in Figure 4, this enzyme catalyzes an intermediate reaction in gluconeogenesis, increasing the overall amount of NAD(P)H in the process without forming CO_2. It is thought that *GDP1* utilizes both NAD^+ and $NADP^+$ with equal affinity – which can be confirmed by the given K_m values for each substrate, as they are within 0.1 mM of

each other – but our preferred use is for NADPH production. Verho et al. also reported lower NADP-GAPDH activity compared to NAD-GAPDH activity when both NAD^+ and $NADP^+$ were present [15].

Figure 4: GAPDH-catalyzed redox reaction where glyceraldehyde-3-phosphate reacts with $NAD(P)^+$ to form 1,3-bisphosphoglycerate and NAD(P)H.

The homologous *pncB* gene (1.2 kb) encodes for an NAPRTase, an enzyme which strongly affects relative amounts of NAD^+ according to the reaction shown in Figure 5 [16]. In theory, increasing the concentration of NAD^+ will effectively increase the overall concentration of all reactants and products in Equation 1 according to LeChatlier's Principle, thus producing the larger amounts of NADPH. The NAPRTase-catalyzed reaction plays an integral role in the NAD^+ salvage pathway – the rate-limiting step. Wubbolts et al. reported a 25-fold increase of *pncB* activity, leading to a 5-fold increase of intracellular NAD when the gene was expressed on a multicopy plasmid in *E. coli*. Other groups report similar results, however, the *pncB* used in their research was heterologous, originating from *Salmonella typhimurium* [17].

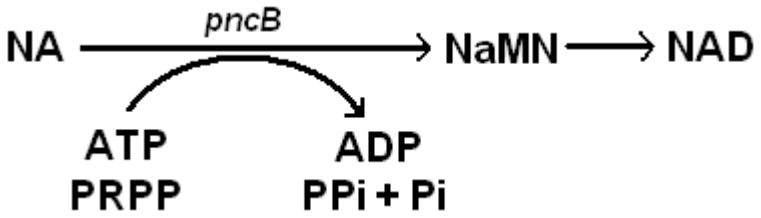

Figure 5: NAPRTase-catalyzed reaction in NAD^+ metabolism where nicotinic acid (NA) reacts with ATP and phosphoribosyl pyrophosphate (PRPP) to form nicotinic acid mononucleotide (NaMN, a direct precursor for NAD^+) and ADP, pyrophosphate (PPi), and phosphate (Pi).

Synthesis of $NADP^+$ from NAD^+ is catalyzed by *nadK*-encoded (0.89 kb) NAD^+ kinase, as shown in Figure 6. This enzyme was partially purified from E. coli by Zerez et al. This group also noted that the activity of *nadK* is regulated by the $NADP^+$/NADPH and NAD^+/NADH ratios [18], and Kawai et al. stated, "NADPH and NADH strongly inhibited the activity of NAD kinase [19]." Observing Equation 1 once again, this phosphorylation clearly causes the reaction to be driven toward the left as the concentration increase of a product (on the right side) throws off the equilibrium, therefore increasing the levels of NADPH in the system to regain balance. Research has shown that overexpression of *nadK* increases the intracellular NADPH/$NADP^+$ ratio [20].

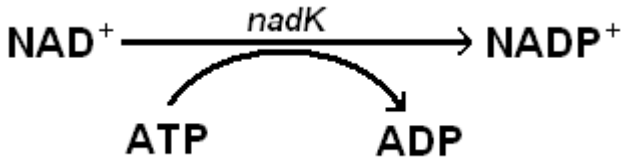

Figure 6: NAD^+ kinase-catalyzed phosphorylation of NAD^+ via reaction with ATP.

The intention of this project was to utilize a biosynthetic system to overexpress chosen enzymes which increase the availability of NADPH and ultimately achieve a higher xylitol yield than previously reported. The W3110-derived base strain PC09 (*crp** and *ΔxylB*) was used, allowing for simultaneous glucose and xylose uptake and disruption of xylose metabolism. Using plasmid pLOI3815, which contained CbXR, as the control plasmid (see Figure 7), the genes previously discussed (*GDP1*, *pncB*, and *nadK*) were inserted immediately downstream of the CbXR gene, creating three novel bicistronic plasmids (pPCC121, pPCC209, and pPCC213, respectively).

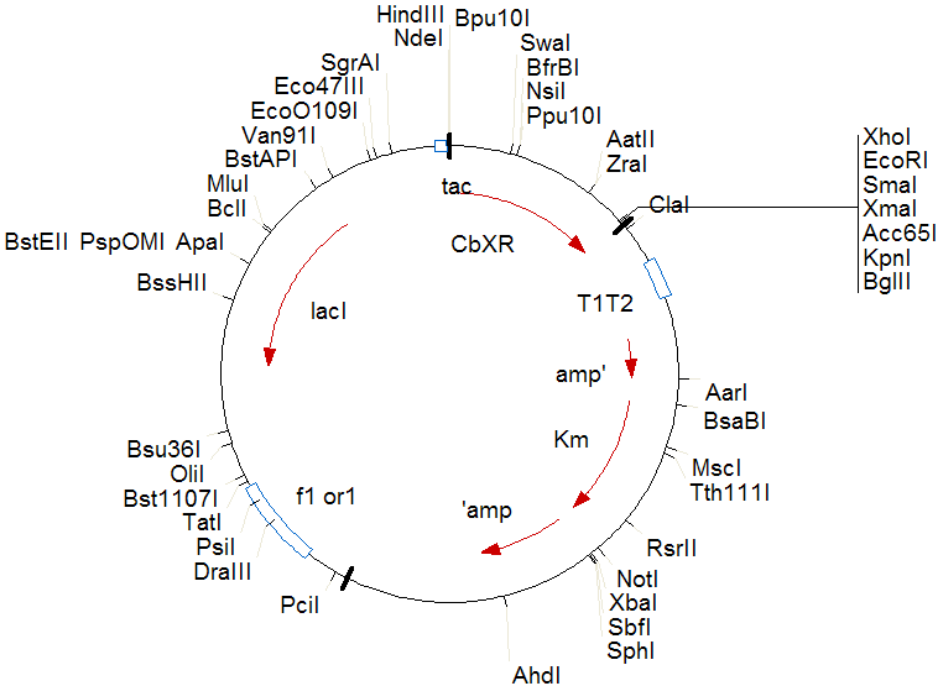

Figure 7: Plasmid pLOI3815, used as a vector for genes encoding enzymes examined in this project.

Several parameters were measured and examined over the course of this research to determine the effects of expressing these enzymes in our *E. coli* system. Overall

xylitol production, glucose and xylose consumption, and acetate and xylulose secretion were closely observed throughout batch culture and resting cell culture experiments. Next, the molar yield of xylitol produced per glucose consumed was compared between enzymes expressed in resting cell cultures. Finally, the cofactor levels were monitored and compared between enzymes via two separate cofactor assay experiments. The analysis of these experiments should better inform us of whether the chosen enzymes are "positively" affecting the system by increasing the NADPH availability and Y_{RPG}.

2. MATERIALS AND METHODS

2.1 Strain and plasmid preparation

For all batch culture and resting cell culture experiments, PC09 acted as the host strain in which the enzymes were overexpressed. PC09, derived from wild type *E. coli* W3110, was constructed according to [10]. It contains two mutations – *crp** and *ΔxylB* – allowing for simultaneous glucose and xylose uptake and inhibition of xylose metabolism, respectively.

The base plasmid, pLOI3809, has pBR322 origin and kanamycin resistance under the control of the *tac* promoter. CbXR was inserted into pLOI3809 to generate pLOI3815, also described in [10]. Both of these plasmids were provided by the Cirino group, while six others were constructed specifically for this project. The gene inserted in each plasmid is listed in Table 1. Among the six plasmids constructed for this research, only the three containing CbXR were used for data analysis while the other three served as controls for the second gene. It should be noted that in the bicistronic plasmids, CbXR was always immediately upstream of the second inserted gene.

Table 1: Summary of Plasmids

Plasmid	**Description**
pLOI3809	Control
pLOI3815	CbXR
pPCC120	*GDP1*
pPCC121	CbXR+*GDP1*
pPCC208	*pncB*
pPCC209	CbXR+*pncB*
pPCC212	*nadK*
pPCC213	CbXR+*nadK*

The *GDP1* gene used to create pPCC120 was amplified from plasmid p1696, a kind gift from Dr. Peter Richard [15]. The polymerase chain reaction (PCR) required more template DNA than usual (4 μL) , as well as a high-fidelity DNA polymerase (*taq*, Phusion). *GDP1*-specific primers were developed with the following sequences:

- GDP1fwd: 5' –AGT CTA CTC GAG AGG AGG ATA GCT CAT GCC CGA TAT GAC AAA CGA – 3'
- GDP1rev: 5'–TGC ACT CCC GGG AAG CGT CTC CTT AAA CAC CAG C–3'

These primers contain the appropriate restriction sites (underlined: *XhoI* and *XmaI*) for ligation into the multiple cloning site of pLOI3809 vector, preceding a transcription termination sequence. During the reaction, a temperature decrement of 1°C per annealing cycle was instilled, steadily decreasing from 80 to 66°C. The upper limit of this range was determined by the melting temperature (T_m) of the primer with the lower T_m, as instructed by the Phusion *taq* requirements.

Both the *GDP1* PCR product and the pLOI3809 plasmid were double-digested (simultaneously reacted with two restriction enzymes) with restriction enzymes *XhoI* and *XmaI*, according to standard procedure proposed by [21] cleaned and concentrated with a Zymo kit, and analyzed via gel electrophoresis to ensure the proper regions were chosen for ligation [21]. The remaining steps of this plasmid construction (pPCC120), including ligation, transformation into DH5α, and colony selection were performed according to standard protocol [22].

In the construction of pPCC121, the *GDP1* gene was isolated from a digestion of pPCC120, rather than from p1696, with the same restriction enzymes noted above. With the exception of pLOI3815 replacing pLOI3809 as the plasmid vector, the same ligation

and ensuing plasmid construction procedures were followed again, with the *GDP1* gene inserted immediately downstream of the CbXR sequence in pLOI3815.

Both *nadK* and *pncB* genes were amplified from an *E. coli* wild-type strain, W3110 [23]. All four plasmids were constructed at the same time, "inserting" each gene into both pLOI3809 and pLOI3815 individually by double digesting with the same restriction enzymes and ligating the gene sequences with the open vectors. The PCR protocol was adjusted slightly in regards to the annealing temperature range, this time decreasing from 73 to 56°C, a decrement of 0.5°C per cycle. The same DNA polymerase was used, with the primer sequences as follows [23]:

- NadK for: 5' – CGC GAG AAT TCA GGA GGA CAG CTA TGA ATA ATC ATT TCA AGT G – 3'
- NadK rev: 5' – CCG CGG GTA CCT TAG AAT AAT TTT TTT GAC CAG CCG AGC TTG GTG C – 3'
- PncB for: 5' – CGC GAG AAT TCA GGA GGA CAG CTA TGA CAC AAT TCG CTT CTC C – 3'
- PncB rev: 5' – CCG CGG GTA CCT TAA CTG GCT TTT TTA ATA TGC GGA AGG TCG – 3'

2.2 Shake Flask Cultures

Shake flask cultures for xylitol production – performed as previously described [10] – contained 50 mL medium in 250-mL baffled flasks and were grown at 30°C and 250 rpm. All LB cultures were supplemented with kanamycin resistance and inoculated to an initial OD_{600} of 0.1 from seed cultures of the same medium. Seed cultures were

prepared by inoculating 3 mL of medium (13 x 100 mm tube) with a streak of colonies from a fresh LB plate (also supplemented with kanamycin). Seeds were grown to an OD_{600} of 2.0-4.0, and shake flask cultures were inoculated directly from the seed cultures by a dilution to a final OD_{600} of 0.1. Enzyme expression was induced with 100 or 300 μM IPTG in shake flasks at the time of inoculation.

2.3 Resting Cells

Resting cells were prepared using a protocol similar to that described in [1], with the exception of the medium being supplemented with kanamycin. Briefly, cells were first grown as 200-mL shake flask cultures (in 1-L flasks) from 25-mL seed cultures (in 250-mL baffled flasks). The 200-mL shake flask culture media contained 100 mM glucose and 50 mM xylose under inducing conditions (100 μM IPTG) with kanamycin resistance (100 μM kan) and MOPS buffer (50 mM). When the OD_{600} was 2.0-4.0, cells were harvested and resuspended to a "working density" of 2.0 in 30-mL minimal medium lacking a nitrogen source and containing 50 mM glucose and 300 mM xylose. Cells were shaken at 30°C and 250 rpm in baffled flasks. Background levels of xylitol production were noted in control experiments in which glucose was not added to the resting cells. This background level of xylitol reduction is perhaps the result of reducing equivalents generated from residual glucose metabolism or biomass degradation. When calculating the molar yield of xylitol, the background level of xylitol produced was taken into account.

2.4 Cofactor Assays

This protocol was developed based on Heuser's method for "Determination of Pyridine Nucleotides in *E. coli* Cell Extracts [16]." To prepare the samples, resting cell cultures at the 24-hour time point were harvested to achieve the equivalent of an OD_{600} of 30.0 in 1 mL. The cell cultures were placed on ice then centrifuged in 50 mL falcon tubes for 10 minutes (3750 rpm, 4°C) and put on ice again. Upon removal of the supernatant, the cells were resuspended and lysed using either 0.5 mL acid (0.3 M HCl supplemented with 50 mM tricine-OH pH 8.0) or base (0.3 M NaOH) and transferred to a microcentrifuge tube. Resuspension required the use of a vortex in both cases, and with NaOH the pellet also needed to be manually broken apart. The cell lysate was incubated at 60°C for 7 minutes, then placed on ice prior to neutralization using either 0.3 M HCl (supplemented with 50 mM tricine-OH pH 8.0) or 0.3 M NaOH. If after neutralization the pH was below 7.0, 100 µL of 1 M tricine-OH pH 8.0 was added. The neutralized cells were centrifuged for another 10 minutes (14,000 rpm, 25°C) and the supernatant was transferred to a clean microcentrifuge tube to be used as a sample for the ensuing assay.

The assay was performed in a 96-well plate. The samples (40 µL oxidized and 40 µL 0.3 M NaCl or 80 µL reduced) were reacted with 100 µL of either an ethanol or glucose-6-phosphate (G6P) solution (prepared with equal volumes of 1.67 mM PES, 40 mM EDTA, 4.2 mM MTT, and 1 M Tricine-NaOH pH 8.0 and either ethanol or G6P). To ensure optimal temperature for the enzyme to catalyze this reaction, the plate was incubated at 37°C for 5 minutes. Next, the wells mixed with ethanol solution were catalyzed by 20 µL alcohol dehydrogenase (ADH), while those including G6P required

20 μL G6P dehydrogenase. The disparity between the ethanol and G6P reaction lies in the specificity of the enzyme – only NAD^+ is reduced by the ethanol/ADH reaction, while only $NADP^+$ is reduced by the G6P/G6PDH reaction. An example of the reaction catalyzed by ADH is shown in Figure 8.

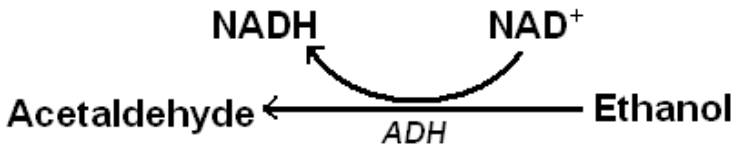

Figure 8: Cofactor Assay oxidation of ethanol to acetaldehyde catalyzed by alcohol dehydrogenase (ADH) to reduce NAD^+ to NADH.

The amount of reduced cofactor produced (and that of oxidized cofactor remaining in the system) was calculated by measuring the formation of reduced MTT with a SpectraMax^{384} mass spectrometer at 30°C and a wavelength of 570 nm. Measurements were taken over a 10 minute time frame in 15 second intervals. Control wells contained varying concentrations of the 'standards' – NAD($^+$/H) and NADP($^+$/H) diluted with NaCl. The dilutions covered the expected range of concentrations from the sample reactions. The appropriate ranges were estimated for the first cofactor assay, and these numbers were adjusted for the duplicate assay to achieve a more accurate calibration curve.

3. RESULTS

3.1 Overall Xylitol Production

The tested plasmids listed in Table 1 (pLOI3815, pPCC121, pPCC209, and pPCC213) were all transformed into PC09 (*crp** and Δ*xylB*)and tested for xylitol production in 50-mL shake flask cultures – grown at 30ºC in LB containing both glucose (100 mM) and xylose (300 mM), and the culture was buffered with MOPS (50 mM). Figure 9 represents the xylitol production profile in each culture over a 96-hour period. "A" indicates samples that were induced with 100 µM IPTG, whereas "B" samples were induced with 300 µM IPTG. Although 100 µM IPTG was sufficient in previous studies [10], it was necessary to verify that the amount of IPTG was not limiting the reduction of xylose to xylitol in the bicistronic plasmids being studied in this project. All of the samples induced with only 100 µM IPTG produced more xylitol than their 300 µM counterpart. The overall production of xylitol after 96 hours was highest when only CbXR was expressed with 100 µM IPTG, reaching ~265 mM (14.4 g xylitol/(g cdw)). The expression of CbXR+*nadK* was the next most productive in terms of total xylitol titer for both inductions, with ~252 mM xylitol in the "A" sample and ~222 mM produced by the "B" sample.

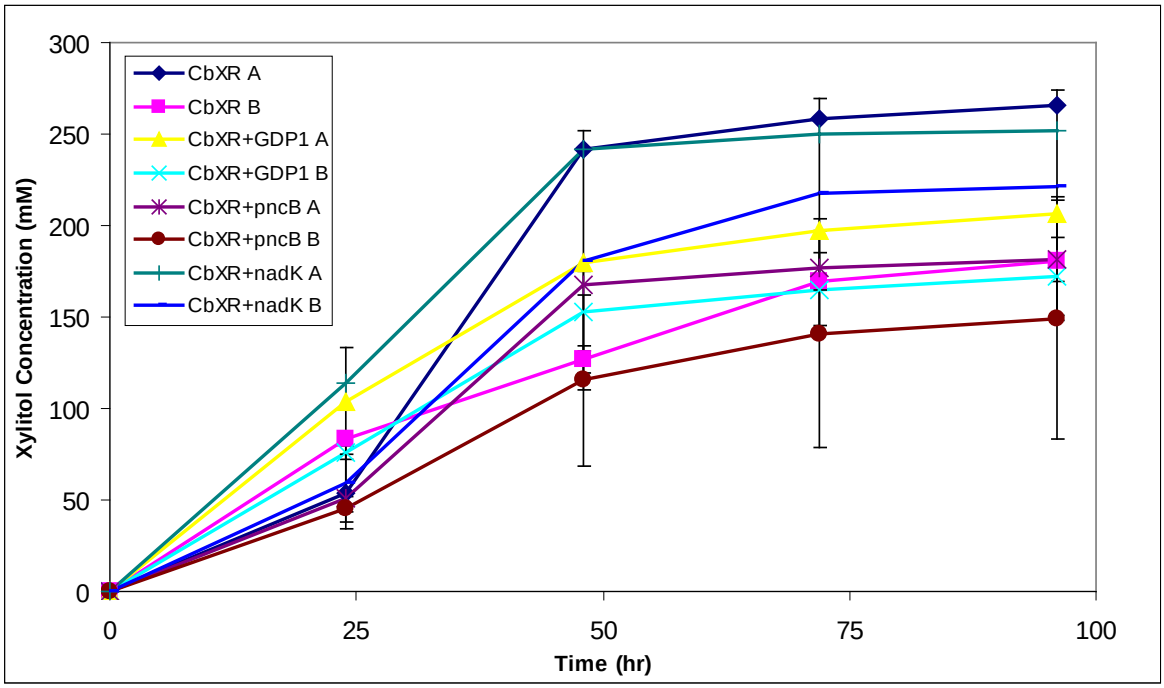

Figure 9: Xylitol production in 50-mL shake flask cultures of strain PC09 harboring the plasmids expressing enzymes tested in this study. Cultures contained xylose (300 mM), glucose (100 mM), MOPS (50 mM), kanamycin (50 µg/mL), and IPTG (100 µM in "A" samples and 300 µM in "B" samples).

It should be noted that after 48 hours, the shake flask cultures induced with 100 µM IPTG had already run out of glucose. This occurred between 48 and 72 hours for those induced with 300 µM IPTG. Since all samples had used up the main source of energy before the data at the final two time points were measured, the growth of the cells and production of xylitol was also carefully viewed over the first 48-hour time period rather than comparing the xylitol production at the 96-hour timepoint. A close-up of the xylitol profile during the first 48 hours can be seen in Figure 10. As it turns out, a slightly different order of samples produced the most xylitol in the earlier stages of the culturing. After 24 hours, the sample expressing *nadK* induced with 100 µM IPTG had already produced ~115 mM xylitol (8 g xylitol/g DW cell), with that expressing GDP1 not far behind at ~105 mM xylitol.

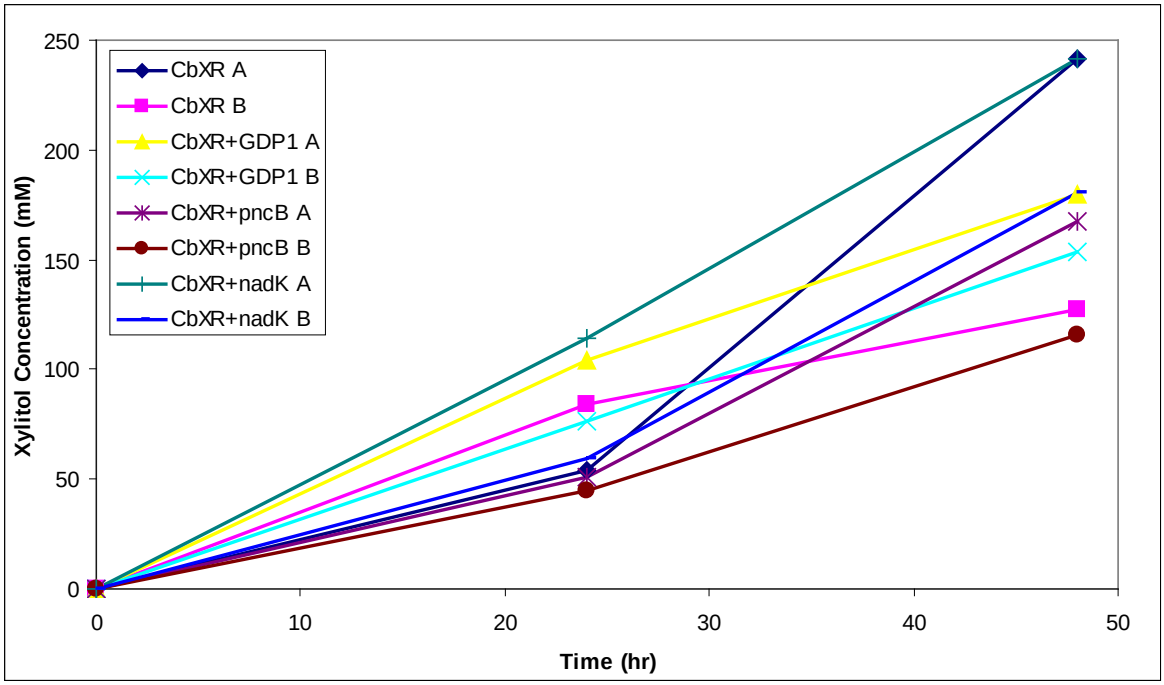

Figure 10: Xylitol production profile, focused on the first 48 hours of the same 50-mL shake flask culture shown in Figure 9. Cultures contained xylose (300 mM), glucose (100 mM), MOPS (50 mM), kanamycin (50 µg/mL), and IPTG (100 µM in "A" samples and 300 µM in "B" samples).

To determine the impact of the number of cells in the shake flask culture versus that of the overexpression of varying enzymes on the levels of xylitol in the first 48 hours, the specific production of xylitol in each sample was calculated. This was done by calculating the amount of xylitol per dry weight of cells (g xylitol / g cdw), which can be converted from the measured OD_{600} at that time point. It is interesting to note that the CbXR "B" sample with the highest specific productivity, produced levels of xylose lower than those in "A" samples expressing *nadK* and *GDP1*. Also, the specific production of xylitol in the "B" sample expressing *nadK* was relatively high, whereas the levels of xylitol seen in Figure 9 were somewhat lower. Overall, the four samples that produced

significantly higher levels of xylitol after 24 hours did have the highest specific productivity.

Table 2: The specific production of xylitol calculated from the 24-hour time point in the 50-mL shake flask culture profiled in Figures 9 and 10.

Expression Characteristic	Concentration IPTG (µM)	Specific Production (g xylitol / g cdw)
CbXR	100	3.6
CbXR+*GDP1*	100	7.1
CbXR+*pncB*	100	3.8
CbXR+*nadK*	100	8.0
CbXR	300	8.6
CbXR+*GDP1*	300	7.4
CbXR+*pncB*	300	4.7
CbXR+*nadK*	300	7.0

Total glucose and xylose consumption as well as xylulose secretion were also compared between the samples induced with 100 µM IPTG and those induced with 300 µM IPTG. There was no difference between sample sets for the total glucose consumed, as the glucose was entirely depleted for all enzymes at both levels of induction. The amount of secreted xylulose for all enzymes was similar between sample sets. Figure 11 shows the comparison of xylose consumption, confirming that 300 µM IPTG was unnecessary in further experiments. In general, the samples induced with 100 µM IPTG consumed all of the xylose provided in the system, while the other samples left close to ~100 mM xylose unconverted.

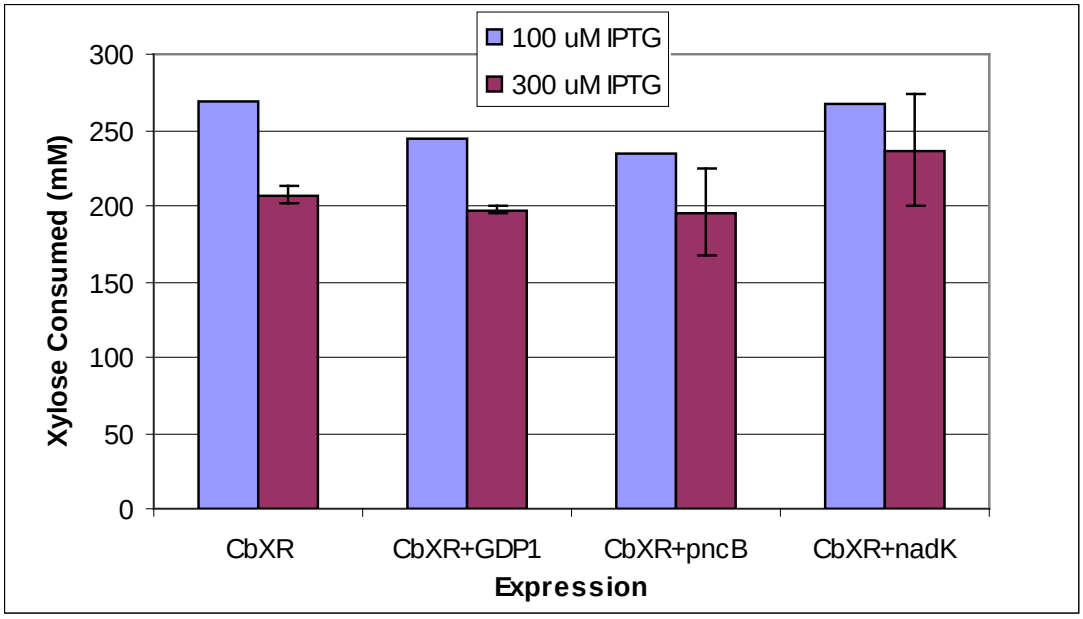

Figure 11: Comparison of total xylose consumed during 96-hour shake flask cultures when samples were induced with 100 µM IPTG or 300 µM IPTG.

Taking a look at another factor thought to contribute to overall xylitol production [10], the acetate secretion profile can be seen in Figure 12. The four samples induced with 300 µM IPTG showed a much higher spike in acetate after 24 hours than any of those induced with 100 µM IPTG. However, after 96 hours there was no clear differentiation between contribution of the two induction levels or the specific enzyme overexpressed in any given sample. While pLOI3815 (CbXR only) did have both the highest overall xylitol production and the lowest acetate secreted, there were no other correlations to be made between the two parameters.

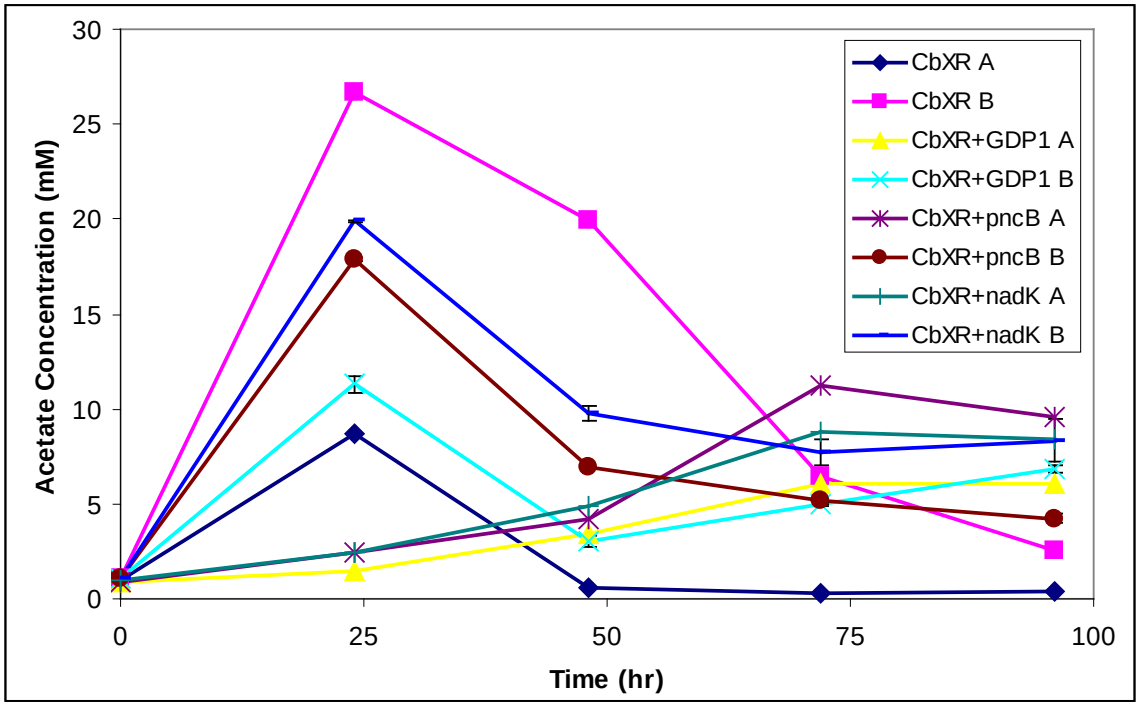

Figure 12: Average acetate excretion profile during 96-hour shake flask cultures. Cultures contained xylose (300 mM), glucose (100 mM), MOPS (50 mM), kanamycin (50 µg/mL), and IPTG (100 µM in "A" samples and 300 µM in "B" samples)

3.2 Xylitol Yield

The molar yield of xylitol per glucose consumed (Y_{RPG}) produced by resting cells was averaged over several data points. This parameter was studied in resting cells, also known as "non-growing" cells, because the lack of nitrogen and/or addition of chloramphenicol do not require glucose and other reducing equivalents to support growth [22]. The results in Figure 13 compared all three enzymes being studied with the "control" (CbXR only), which has been examined in the past. The yields obtained by expressing CbXR in PC09 are within the standard deviation of these previously reported results [10]. Overall, the average Y_{RPG} was highest with *GDP1* expression (3.94±1.08 and 3.39±0.46 at 24- and 48-hour time points, respectively) compared to that of only

CbXR (3.13±0.58 and 2.71±0.39). Y_{RPG} remained fairly constant between expressing only CbXR and expressing CbXR+*nadK* (3.40±1.42 and 3.01±0.61), and Y_{RPG} decreased slightly when CbXR+*pncB* was expressed (2.33±0.74 and 2.57±0.42).

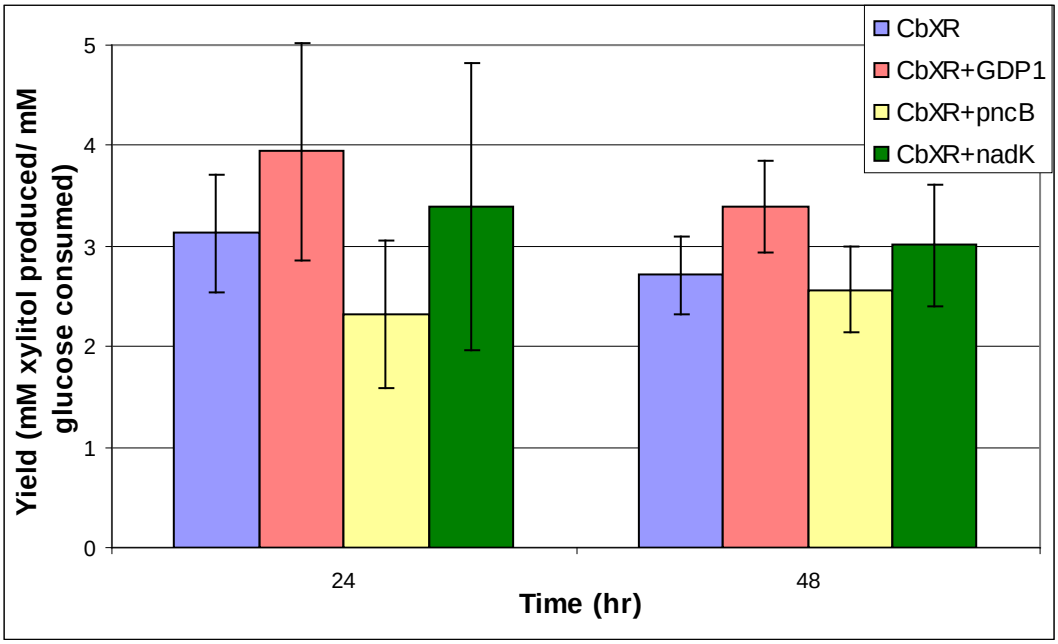

Figure 13: Molar yield of xylitol produced per glucose consumed by resting cells of the noted plasmids overexpressed in PC09. The working cell density (OD_{600}) was 2.0 (in LB medium), and aeration was achieved by shaking at 250 rpm in baffled flasks.

By finding the average Y_{RPG} values the comparisons stated above can be made, however a student t-test shows that the majority of the results obtained are statistically similar at both the 24-hour and the 48-hour time point. Each enzyme was compared individually to CbXR to calculate the p values shown in Table 3. In this study, any p value greater than 10% was chosen to signify statistic similarity between the Y_{RPG} values of each sample.

Table 3: T-test results for Y_{RPG} with each enzyme expressed related to CbXR-only expression.

Gene (+CbXR)	p Value t = 24 hr	p Value t = 48 hr
GDP1	16%	3%
pncB	11%	32%
nadK	39%	22%

3.3 Cofactor Analysis

The intracellular redox environment was examined by measuring the internal nicotinamide cofactor concentrations for PC09 resting cells harboring the four main plasmids in this study (pLOI3815, pPCC121, pPCC209, and pPCC213). The resting cells were suspended in either glucose medium ("-X") or glucose and xylose ("+X") medium. The -X samples better represent levels of NADPH the cell produced without expending energy (via NADPH oxidation) by producing xylitol. The resulting cofactor concentration, quantities, and ratios ($NADH/NAD^+$ and $NADPH/NADP^+$) were compared to one another in addition to being related to the xylitol amounts (g / g cdw) and yields (Y_{RPG}) produced in resting cells expressing the same enzymes.

3.3.1 Cofactor Concentration

By correlating the profile of absorbance measurements from known 'standard' concentrations of cofactor to those measured during the assay reactions, the concentration of all oxidized and reduced nicotinamide cofactors in the system can be determined. The average concentration of each cofactor (NADH, NAD^+, NADPH, and $NADP^+$) from the

assay was calculated. In Figures 14, 15, and 16 the results are shown as an individual comparison of CbXR to CbXR+ *GDP1*, *pncB*, and *nadK*, respectively.

The reaction catalyzed by *GDP1* should convert $NAD(P)^+$ to NAD(P)H, increasing the overall reduced cofactor concentration. Figure 14 illustrates that the reduced cofactor levels did not seem to be impacted by the addition of *GDP1* expression when xylose was present in the medium. Under xylose-limited conditions, NADH concentration was unchanged but that of NADPH dropped and was proven to be statistically differing ($p < 1\%$) between the expressions of each enzyme. On the other hand, the oxidized cofactor concentrations increased under both +/-X conditions.

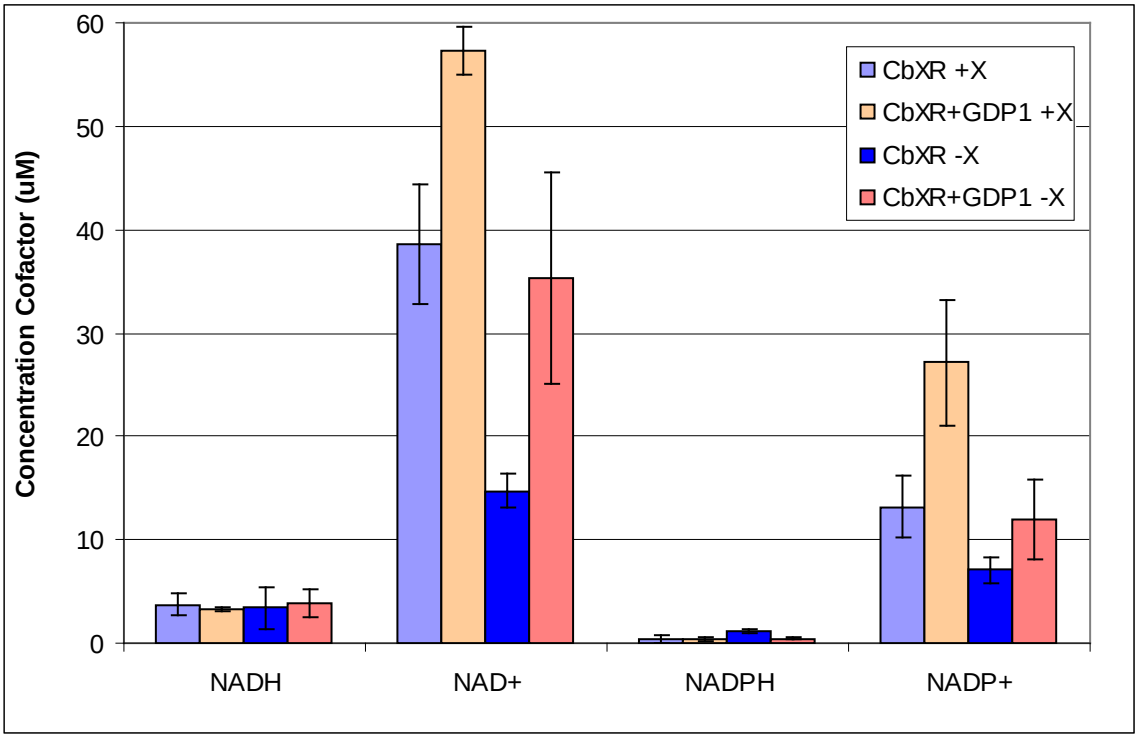

Figure 14: The concentration (µM) of reduced and oxidized nicotinamide cofactors when the cells were expressing only CbXR or CbXR+*GDP1* in either glucose-supplemented media (-X) or that with both glucose and xylose (+X).

The expression of *pncB* was expected to impact the cofactor concentrations by increasing the total amount of NAD^+ in the system. Under xylose-limited conditions, the average concentration of all cofactors increased somewhat, with that of NAD^+ more than doubling. The average concentration of NAD^+ in "+X" samples decreased slightly, but considering the error associated with this data, the difference was not significant.

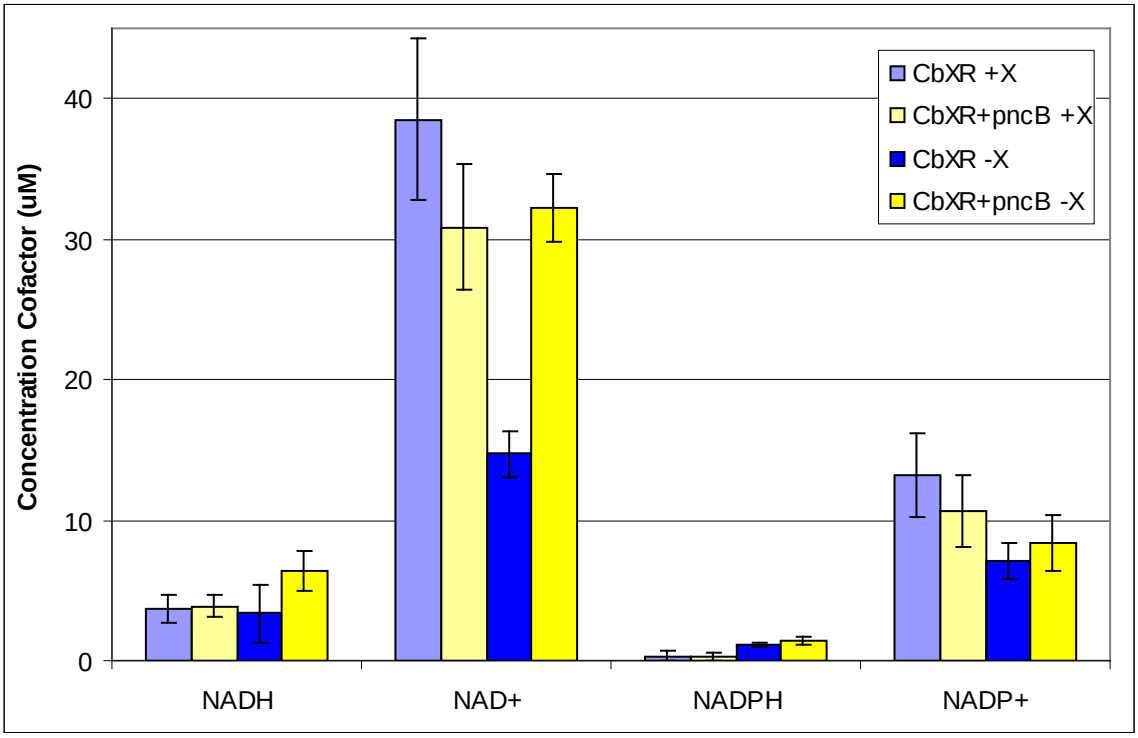

Figure 15: The concentration (µM) of reduced and oxidized nicotinamide cofactors when the cells were expressing only CbXR or CbXR+*pncB* in either glucose-supplemented media (-X) or that with both glucose and xylose (+X).

The concentrations of both NADPH and $NADP^+$ were expected to increase when expressing *nadK* because the kinase phosphorylates the target substrate, NAD^+. Figure 16 verifies that this occurred under both +/-X conditions, with all values proven

statistically different from expression of CbXR only (all $p < 1\%$). In this case, the average concentration of NADH and NAD^+ decreased under +/-X conditions.

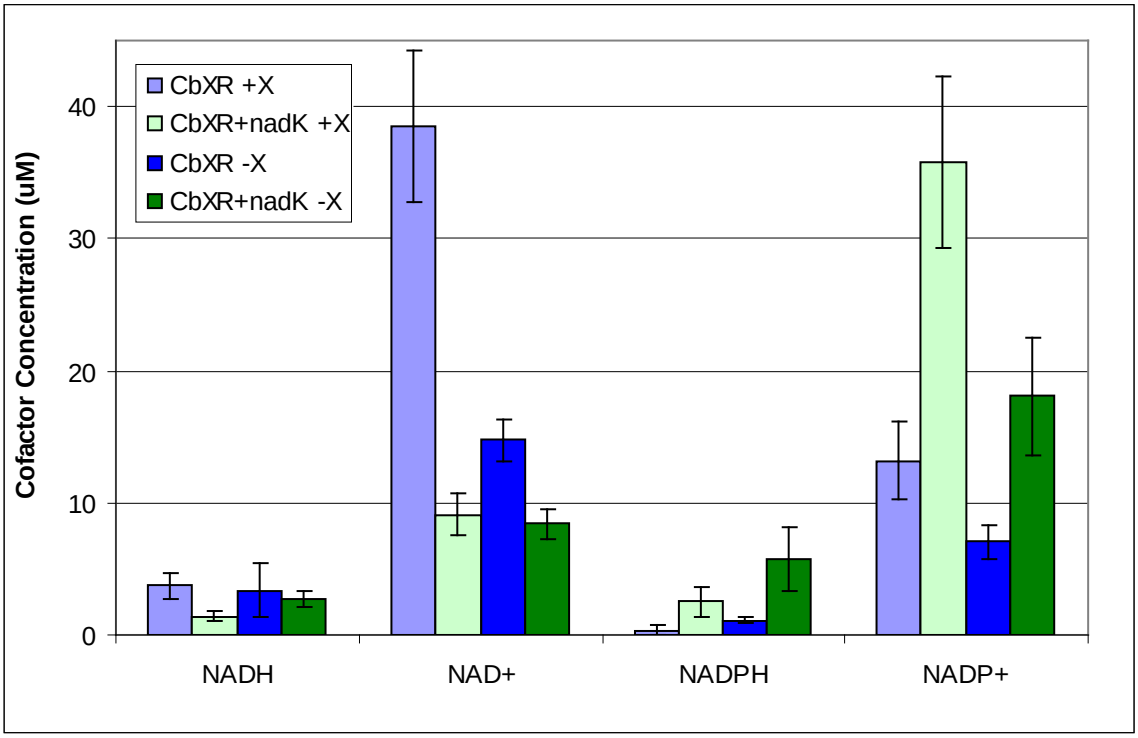

Figure 16: The concentration (µM) of reduced and oxidized nicotinamide cofactors when the cells were expressing only CbXR or CbXR+*nadK* in either glucose-supplemented media (-X) or that with both glucose and xylose (+X).

3.3.2 Cofactor Ratios

From the concentrations, the ratio of reduced to oxidized cofactor ($NADH/NAD^+$ and $NADPH/NADP^+$) was calculated for both +/-X conditions. A complete list of the averaged ratios from the two cofactor assays is presented in Table 4. The ratios of cofactors from samples lacking xylose were consistently higher than those supplemented with xylose. Comparing both ratios between CbXR samples and the other three genes included, only *pncB* produced statistically similar ratios ($p \sim 30\%$). Otherwise, *nadK*

produced statistically higher ratios in both cases, while *GDP1* expression resulted in lower ratios overall.

Table 4: Ratio of reduced to oxidized cofactor from resting cells, in which cells were harvest 24 hours after resuspending in nitrogen-limited medium.

Expression	X (+ / -)	NADH/NAD$^+$	NADPH/NADP$^+$
CbXR	+	0.10 ± 0.04	0.02 ± 0.02
CbXR	-	0.24 ± 0.16	0.16 ± 0.06
CbXR+*GDP1*	+	0.06 ± 0.01	0.02 ± 0.01
CbXR+*GDP1*	-	0.11 ± 0.03	0.04 ± 0.02
CbXR+*pncB*	+	0.13 ± 0.04	0.03 ± 0.03
CbXR+*pncB*	-	0.20 ± 0.06	0.19 ± 0.07
CbXR+*nadK*	+	0.16 ± 0.05	0.07 ± 0.04
CbXR+*nadK*	-	0.33 ± 0.08	0.33 ± 0.16

The comparison between NADPH/NADP$^+$ ratios and Y_{RPG} is shown in Figure 17. Figure 18 depicts the relationship between NADH/NAD$^+$ ratios and Y_{RPG}. The figures each contain two sets of data, representing the xylose-limited samples (referred to as "-X") as well as the difference in NADPH/NADP$^+$ ratio in the absence of xylose minus the same ratio in the presence of xylose (referred to as "Delta"). The "Delta" samples provide insight on the impact attributed solely to xylose reduction. The significant amount of error associated with these ratios by taking the average of so few sets of data allows for no identification of clear correlations in the data.

An increase and decrease in NADPH/NADP$^+$ both increased the average Y_{RPG} in the cases of *nadK* and *GDP1*, respectively. Specifically regarding the statistical analysis, the ratios calculated from CbXR data were proven to be different from those of *nadK* (higher ratios) and *GDP1* (lower ratios), but neither caused a statistically significant change in the overall xylitol yield. The NADH/NAD$^+$ ratios were considered unchanged

by both *pncB* and *nadK* expression (both p > 15%). *GDP1* expression saw ratios only 5% similar to those of CbXR. Again, without the significant error, a slight upward trend can be viewed in Figure 18 with increases in NADH/NAD$^+$ ratios corresponding to increases in xylitol yield.

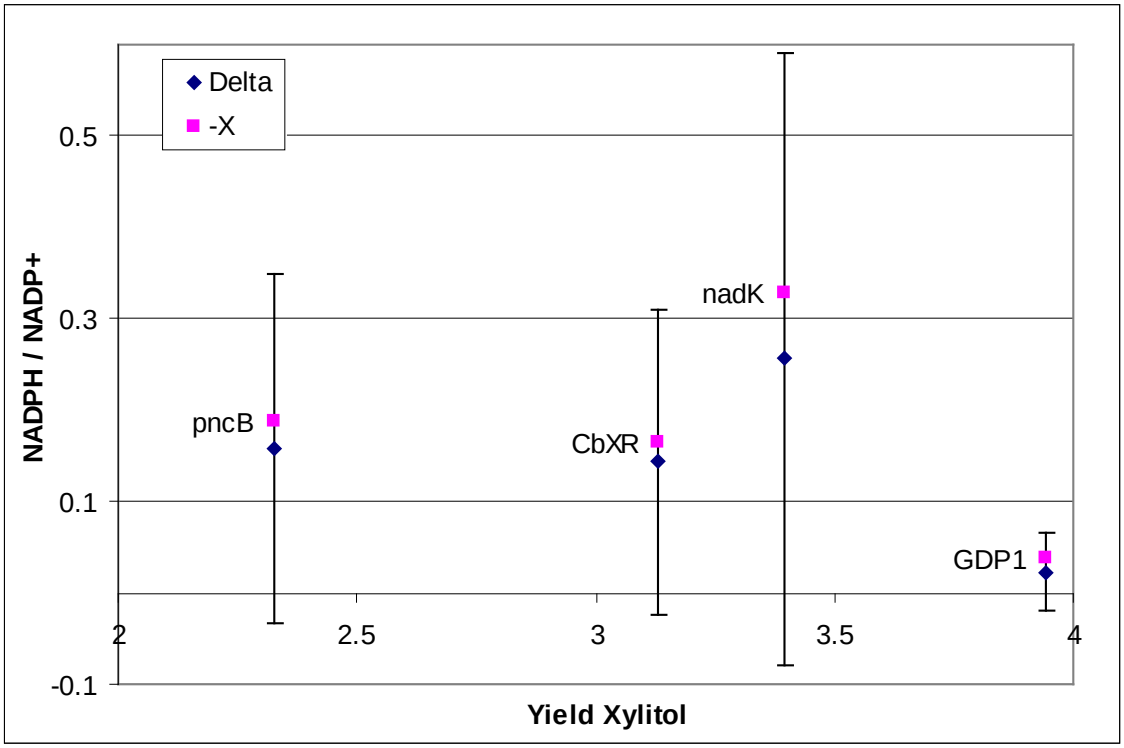

Figure 17: Comparison of NADPH/NADP$^+$ versus xylitol yield (Y_{RPG}). "-X" samples denote those that were cultured in xylose-limited medium. "Delta" samples represent the difference between the ratios in the absence and in the presence of xylose.

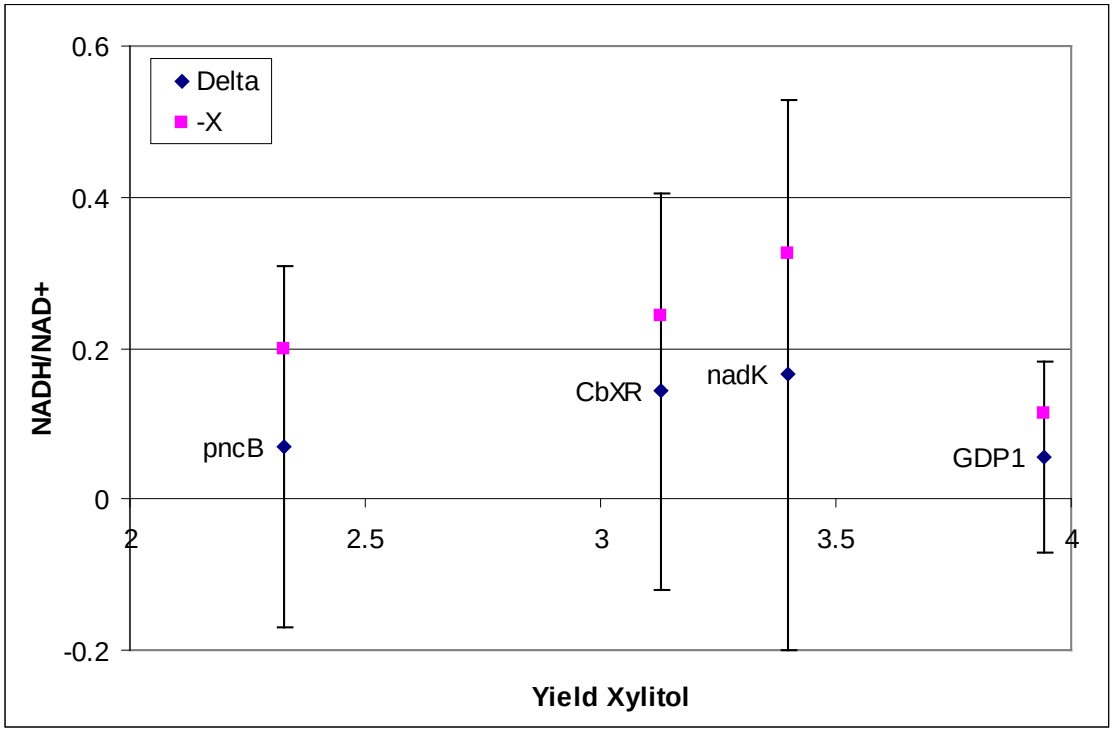

Figure 18: Comparison of NADH/NAD$^+$ versus xylitol yield (Y_{RPG}). "-X" samples denote those that were cultured in xylose-limited medium. "Delta" samples represent the difference between the ratios in the absence and in the presence of xylose.

3.3.3 Total Cofactor

In addition to analyzing the ratio of reduced to oxidized cofactor, the total amount of cofactor (µmol/g cdw) may have changed due to the enzyme expression studies, and these changes may correlate with the overall xylitol yield. Therefore the total amount of NADPH, reduced cofactor (NAD(P)H), and oxidized cofactor (NAD(P)$^+$) were compared to Y_{RPG}. In Table 5, these amounts are reported with their standard deviation. The numbers were calculated directly from the concentration values, with a conversion of (0.33 g cdw / OD_{600}-L). The volume of the reaction was 200 µL (from the cofactor assay reaction procedure), and the sample volume was 80 µL for reduced cofactors or 40 µL for oxidized cofactors.

Table 5: The amount of total NADPH, reduced cofactor (NAD(P)H), and oxidized cofactor ($NAD(P)^+$) reported in µmol/g cdw

Expression	X (+ / -)	NADPH (µmol / g cdw)	NAD(P)H (µmol / g cdw)	$NAD(P)^+$ (µmol / g cdw)
CbXR	+	0.08±0.09	1.02±0.28	26.13±3.29
CbXR	-	0.28±0.05	1.13±0.52	11.01±1.05
CbXR + *GDP1*	+	0.10±0.04	0.94±0.08	42.65±3.29
CbXR + *GDP1*	-	0.11±0.02	1.09±0.33	23.88±5.48
CbXR + *pncB*	+	0.07±0.07	1.05±0.21	20.94±2.60
CbXR + *pncB*	-	0.37±0.07	1.97±0.37	20.50±1.59
CbXR + *nadK*	+	0.63±0.28	0.99±0.29	22.67±2.39
CbXR + *nadK*	-	1.44±0.64	2.13±0.63	13.39±2.34

As discussed previously, the total concentration of NADPH did not differ significantly between expression of CbXR and *pncB*, it decreased with *GDP1* expression, and it increased with *nadK* expression. According to the comparison made in Figure 19, the amount of NADPH did not have a clear impact on the average xylitol Y_{RPG}. Without considering the *nadK* data due to the significant error, a very slight downward trend can be noted, meaning lower total amounts of NADPH resulted in a higher Y_{RPG}. However, since the statistical data for Y_{RPG} between CbXR and other enzymes verified that the values were basically equivalent, this trend cannot be confirmed with the given results.

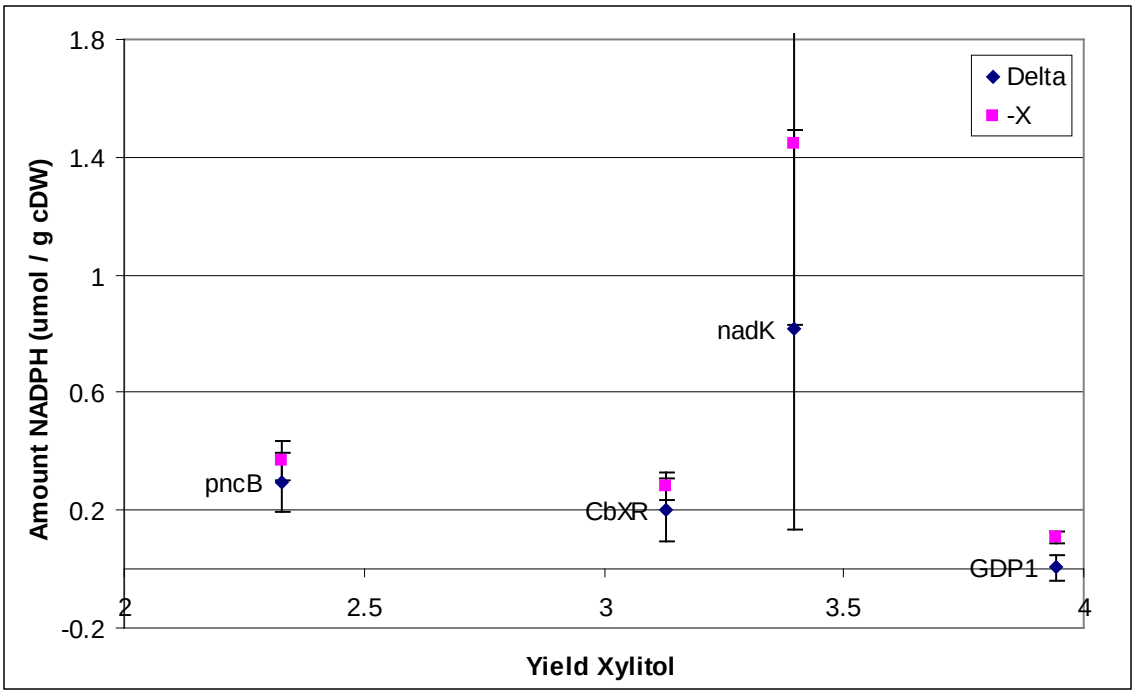

Figure 19: Comparison of the total amount of NADPH produced via expression of different enzymes versus xylitol yield (Y_{RPG}) for xylose-limited (-X) and the difference between NADPH/NADP$^+$ in the absence and presence of xylose (Delta).

The total amounts of reduced cofactor, NAD(P)H, and oxidized cofactor, NAD(P)$^+$, are plotted against Y_{RPG} in Figures 20 and 21, respectively. In calculating total amount of NAD(P)H, the error associated with each data point does not allow for conclusive tendencies to be seen in the comparison. While the average levels of total reduced cofactor were slightly higher than CbXR with *pncB* and *nadK* expression, *GDP1* did not alter the levels at all.

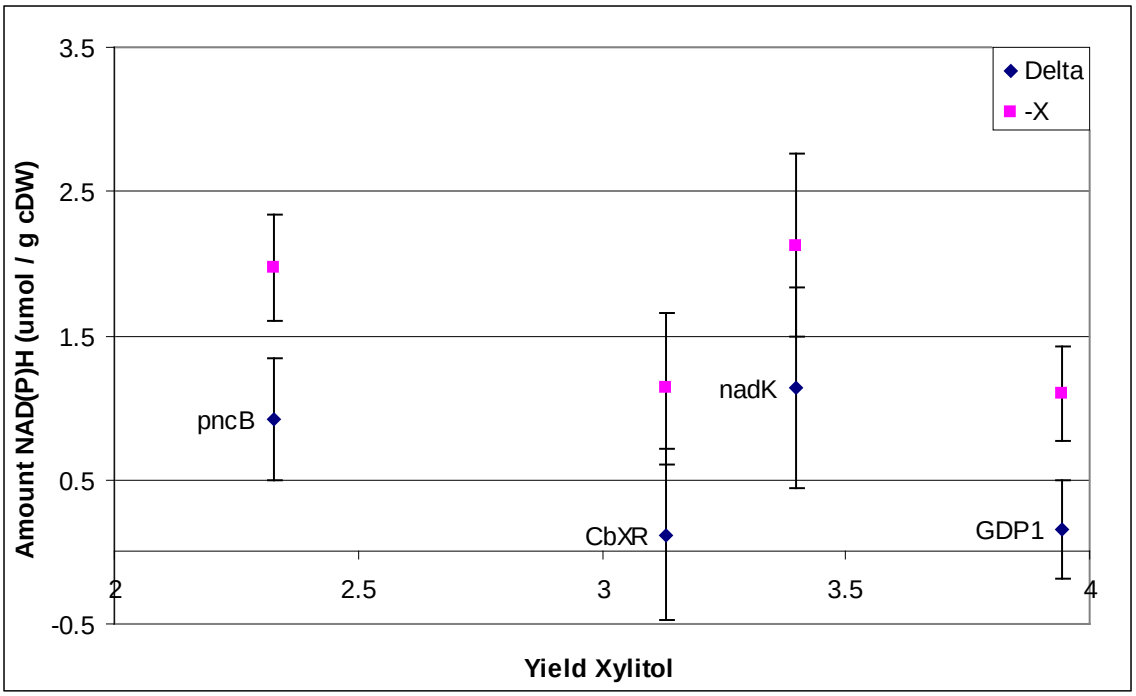

Figure 20: Comparison of the total amount of reduced cofactor, NAD(P)H, produced via expression of different enzymes versus xylitol yield (Y_{RPG}) for xylose-limited (-X) and the difference between NADPH/$NADP^+$ in the absence and presence of xylose (Delta).

In Figure 21, the "+X" data set – representing the results from samples containing both glucose and xylose in the resting cell state – replaces the "Delta" data set found elsewhere throughout this study. In the case of oxidized cofactor, the lack of xylose in the system does not increase the total amount as it does with reduced cofactor levels. With slightly less error in the second data set, levels of oxidized cofactor are generally shown to positively correlate with Y_{RPG}.

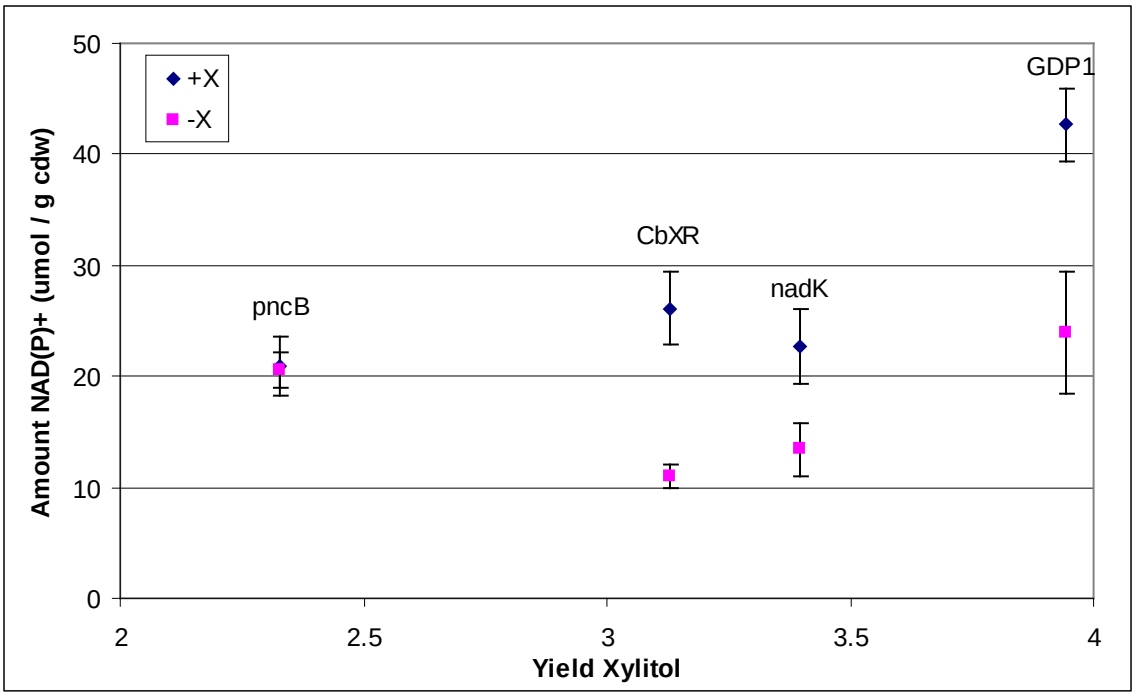

Figure 21: Comparison of the total amount of oxidized cofactor, $NAD(P)^+$, produced by expressing different enzymes versus xylitol yield (Y_{RPG}) for media either supplemented (+X) or lacking (-X) xylose.

4. DISCUSSION & RECOMMENDATIONS

In the case of all three genes expressed on bicistronic plasmids, the yield of xylitol produced per glucose consumed was considered to be no different than that found by expressing only CbXR in the same system as has been studied in the past. The data produced in this study for CbXR Y_{RPG} was similar to results previously reported, so our Y_{RPG} can be accurately compared. To achieve more conclusive results, more data needs to be collected to reduce the error associated with the Y_{RPG} calculated from resting cell cultures harboring each novel plasmid. With a smaller standard deviation, *nadK* expression in particular could allow for a higher Y_{RPG} as a result of increasing the ratio of $NADPH/NADP^+$ as expected.

4.1 *GDP1 Expression*

In general, the Y_{RPG} values found by culturing with *GDP1* present in addition to CbXR were statistically the least similar of the three enzymes compared to CbXR. Table 3 shows that the average Y_{RPG} value calculated from the 48-hour time point data was actually different. However, the inconsistency in statistical difference between time points makes it difficult to prove that Y_{RPG} has indeed increased due to *GDP1* expression. Especially considering the high xylitol production observed in batch culture results, it would be beneficial to collect several more data sets and decrease the error associated with the current Y_{RPG} values because of the statistical results for the ratios for both $NADPH/NADP^+$ and $NADH/NAD^+$. With both ratios considered significantly lower than those seen in CbXR expression, it would be interesting to see whether or not the ratios would have an impact on a more reliable Y_{RPG} value.

Analysis of the difference in concentration of each cofactor (reduced and oxidized) provides some insight as to what may be occurring in the system. As noted previously, the oxidized cofactor levels increased, while the reduced cofactor levels remained constant when expressing CbXR+*GDP1* as opposed to only CbXR. With the extra burden on the cell posed by the synthesis of a second protein, encoded by *GDP1*, it is likely that the cell naturally synthesized excess oxidized cofactor during growth. Upon initiation of the resting state, when cells were deprived of a nitrogen sources and chloramphenicol was added to suppress further metabolism, only a stoichiometric amount of reduced cofactor can be produced. Basically, the cell could have already 'maxed out' the amount of reduced cofactor able to be produced, even though there was plenty more oxidized cofactor available in the system.

The cell's use of homologous *gapA* instead of heterologous *GDP1* poses another plausible scenario. As shown in Figure 22, *gapA* encodes for an enzyme that catalyzes the same reaction in glycolysis as the *GDP1*-encoded enzyme, with the exception that it utilizes NAD^+ preferentially. The enzymes encoded by *gapA* and *GDP1* have similar affinities for glyceraldehyde-3-phosphate in wild-type *E. coli* ($K_{m,gapA}$ = 0.89 mM [24] and $K_{m, GDP1}$ = 0.75 mM [15]). However, *gapA* GAPDH has a much higher affinity for NAD^+ than *GDP1* GAPDH does for $NADP^+$ ($K_{m, gapA}$ = 0.045 mM [24] and $K_{m, GDP1}$ = 0.40 mM [15]). Combining this kinetic data with the increased NAD^+ availability seen in the concentration levels, there is a chance that *GDP1* expression was not actually the cause for yield and cofactor levels seen in the resting cell and cofactor assay experiments. To test for enzymatic activity while expressing *GDP1*, GAPDH assays have been performed and reported by several groups already [15, 25, 26].

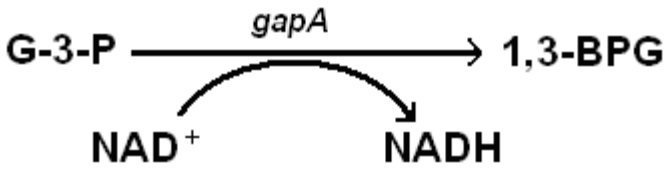

Figure 22: GAPDH-catalyzed redox reaction where glyceraldehyde-3-phosphate reacts with NAD^+, and does not use $NADP^+$ as a cofactor, to form 1,3-bisphosphoglycerate and NADH.

Replacement of the *gapA* gene encoding an NAD-GAPDH with *gapC*, an NADP-GAPDH from *Clostridium acetobutylicum*, was successfully accomplished by Martinez et al [26]. They constructed two Δ*gapA* strains of *E. coli* in which they then overexpressed the *gapC* gene, resulting in an overall increase in NADPH availability because during glycolysis the system consistently generated NADPH instead of NADH. In the hopes of recreating these results, construction of a Δ*gapA* strain of *E. coli* was attempted with the plan of then overexpressing *GDP1*, but issues arose with cell growth on regular LB agar plates. It was discovered that the strains lacking a *gapA* gene could only be sustained on minimal-media plates with specific supplements, and these were not constructed for this project.

Successful deletion of the *gapA* gene encoding for an NAD-dependent GAPDH would likely improve our *GDP1*-expressing system. Following a similar thought process as Verho et al., *GDP1* could be integrated into the chromosome, thus ensuring the glycolysis production of NADPH rather than NADH.

4.2 *pncB Expression*

Expression of *pncB* produced the lowest overall xylitol production seen in batch culture results as well as a lower average Y_{RPG} value than CbXR expression. As with *GDP1*, *pncB* expression produced one statistically similar Y_{RPG} value, although in this case it was at the 48-hour time point. The inconsistency still applies, and the data and error still need much improvement before any reliable conclusions can be stated. Additionally, both cofactor ratios (NADPH/$NADP^+$ and NADH/NAD^+) were proven to be statistically similar to those seen in CbXR expression. With the multiple cases of statistical similarity, the additional expression of *pncB* cannot yet be considered any different from the previous system seen with CbXR.

As noted previously, the dramatic increase in NAD^+ concentration levels was seen with the expression of *pncB* in the xylose-limited system. However, this trend was also seen under *GDP1*-expression conditions. The same explanation could apply to *pncB* as well, with the extra burden on the cell of synthesizing a second protein causing the oxidized cofactor levels to increase. The NADPH levels were also improved in this system, but the cofactor regeneration in this system cannot be considered to have changed much from previously studied systems.

Other studies focused on overexpressing the *pncB* gene achieved consistently higher NADN/NAD^+ ratios as well as overall levels of NAD(H) [17, 27, 28]. The amount of NAD^+ (μmol/g cdw) found in this study was merely half that seen by Wubbolts et al. when they introduced multiple copies of a plasmid harboring the same homologous gene. Since results comparable to previous studies under similar conditions were not achieved, it would be necessary to examine the activity of the enzyme to be sure

it was catalyzing specific reactions as expected. A few other groups have performed this activity assay and reported results that could be compared to an assay performed for this purpose [17, 28].

4.3 *nadK Expression*

The expression of *nadK* allowed for an increase in overall xylitol production in batch cultures as well as a slightly higher Y_{RPG} value. Unfortunately, the Y_{RPG} value was not proven to be statistically different from that seen from CbXR expression, as the t-test p value at both time points greater than 20%. With more data collected under *nadK* expression, a smaller error and more reliable yield could be achieved.

NAD^+ kinase showed the most interesting results in regards to the cofactor assay analysis. As expected, the concentration levels for oxidized and reduced phosphorylated cofactors under both +/-X conditions saw a substantial increase while all non-phosphorylated levels decreased slightly. Without the activity analysis for this enzyme, the impact on these concentration levels are our only way of justifying that the kinase was being expressed to some extent in the system.

Additionally, the NADPH/$NADP^+$ ratio nearly doubled with *nadK* expression – increasing from 0.143 to 0.256 – with the NADH/NAD^+ ratio remaining constant. Similarly, Lee et al. reported an increase in NADPH/NADP+ from 0.184 to 0.267 [20]. One variation seen from their results was an overall increase in $NADP^+$ levels when they reported 10% decreases, yet the ratios were consistent.

The parallels between the cofactor results seen in our study and those of other groups lead us to believe that the expression of this enzyme should have a greater impact

on the Y_{RPG} value because of the boosted NADPH availability. If the average yield were to remain higher than that seen by expressing CbXR, a positive correlation could be made between nadK expression, NADPH availability, and xylitol produced per glucose consumed. To properly examine the activity of the enzyme being expressed, appropriate *nadK* activity assays are reported by Kawai et al. and Lee et al [19, 20] with protocols that should allow for assessment of the activity of each enzyme.

4.4 Other Recommendations

There are a few other additions and changes that can be made to improve this study and confirm the thought that these enzymes can improve the xylitol production and yield in whole-cell biocatalysis. Most importantly, the experiments conducted and reported in this paper should be repeated several more times to decrease the error found.

The only additional experimentation not covered in this study is the enzymatic activity assays discussed previously. Many of the assays reported by other research groups can be recreated and analyzed for our specific systems. With this proof of activity, we can at least conclude that the results are linked to the expression of the enzymes in this study. Otherwise, many of the results obtained may be attributed to lack of activity of the designated enzyme.

Further studying the level of induction with different concentrations of IPTG may also be useful. Although it was determined that the 100 µM IPTG induction was sufficient, there were not multiple batch cultures run at both 100 and 300 µM IPTG to be fully confident in this assessment. If this were to limit growth or xylose reduction at all, this would definitely impact the results seen in xylitol yield.

5. CONCLUSIONS

The results reported in this study must be considered inconclusive due to the large error associated with most of the data. The yield of xylitol seen with *GDP1* and *nadK* expression is promising, but more resting cell culture data is necessary to prove that Y_{RPG} is not the same as seen by expressing CbXR. The overall xylitol production and average Y_{RPG} values reported under the expression of these two genes were higher than that of CbXR, so there is potential for a more efficient system to produce xylitol in larger quantities. According to the reported results thus far, it does not seem that *pncB* expression improves the system compared to CbXR.

Cofactor assays for both of these enzymes need to be repeated to verify the NADPH levels as well as the cofactor ratios. Since Cirino et al. have seen in the past that an increase in these two parameters has positively affected xylitol yield, we need to confirm the levels by reducing the error associated with the data in this study because trends were noticed in the opposite direction.

6. REFERENCES

1. Chin, J.W., et al., *Analysis of NADPH Supply During Xylitol Production by Engineered Escherichia coli.* Biotechnology and Bioengineering, 2009. **102**(1): p. 209-220.
2. Akinterinwa, O., R. Khankal, and P.C. Cirino, *Metabolic engineering for bioproduction of sugar alcohols.* Current Opinion in Biotechnology, 2008. **19**(5): p. 461-467.
3. van der Donk, W.A. and H.M. Zhao, *Recent developments in pyridine nucleotide regeneration.* Current Opinion in Biotechnology, 2003. **14**(4): p. 421-426.
4. Schmid, A., et al., *Industrial biocatalysis today and tomorrow.* Nature, 2001. **409**(6817): p. 258-268.
5. Duetz, W.A., J.B. van Beilen, and B. Witholt, *Using proteins in their natural environment: potential and limitations of microbial whole-cell hydroxylations in applied biocatalysis.* Current Opinion in Biotechnology, 2001. **12**(4): p. 419-425.
6. Granstrom, T.B., K. Izumori, and M. Leisola, *A rare sugar xylitol. Part I: the biochemistry and biosynthesis of xylitol.* Appl Microbiol Biotechnol, 2007. **74**(2): p. 277-81.
7. Granstrom, T.B., K. Izumori, and M. Leisola, *A rare sugar xylitol. Part II: biotechnological production and future applications of xylitol.* Appl Microbiol Biotechnol, 2007. **74**(2): p. 273-6.
8. Parajo, J.C., H. Dominguez, and J.M. Dominguez, *Biotechnological production of xylitol. Part 1: Interest of xylitol and fundamentals of its biosynthesis.* Bioresource Technology, 1998. **65**(3): p. 191-201.
9. Nigam, P. and D. Singh, *Processes for Fermentative Production of Xylitol - a Sugar Substitute.* Process Biochemistry, 1995. **30**(2): p. 117-124.
10. Cirino, P.C., J.W. Chin, and L.O. Ingram, *Engineering Escherichia coli for xylitol production from glucose-xylose mixtures.* Biotechnology and Bioengineering, 2006. **95**(6): p. 1167-1176.
11. Kotter, P. and M. Ciriacy, *Xylose Fermentation by Saccharomyces-Cerevisiae.* Applied Microbiology and Biotechnology, 1993. **38**(6): p. 776-783.
12. Khankal, R., et al., *Transcriptional effects of CRP* expression in Escherichia coli.* J Biol Eng, 2009. **3**: p. 13.
13. Khankal, R., J.W. Chin, and P.C. Cirino, *Role of xylose transporters in xylitol production from engineered Escherichia coli.* J Biotechnol, 2008. **134**(3-4): p. 246-52.
14. Sauer, U., et al., *The soluble and membrane-bound transhydrogenases UdhA and PntAB have divergent functions in NADPH metabolism of Escherichia coli.* Journal of Biological Chemistry, 2004. **279**(8): p. 6613-6619.
15. Verho, R., et al., *Identification of the first fungal NADP-GAPDH from Kluyveromyces lactis.* Biochemistry, 2002. **41**(46): p. 13833-13838.
16. Heuser, F., et al., *Enhancement of the NAD(P)(H) pool in Escherichia coli for biotransformation.* Engineering in Life Sciences, 2007. **7**(4): p. 343-353.
17. San, K.Y., et al., *Metabolic engineering through cofactor manipulation and its effects on metabolic flux redistribution in Escherichia coli.* Metabolic Engineering, 2002. **4**(2): p. 182-192.

18. Zerez, C.R., et al., *Negative Modulation of Escherichia-Coli Nad Kinase by Nadph and Nadh.* Journal of Bacteriology, 1987. **169**(1): p. 184-188.
19. Kawai, S., et al., *Molecular characterization of Escherichia coli NAD kinase.* European Journal of Biochemistry, 2001. **268**(15): p. 4359-4365.
20. Lee, H.C., et al., *Thymidine production by overexpressing NAD(+) kinase in an Escherichia coli recombinant strain.* Biotechnology Letters, 2009. **31**(12): p. 1929-1936.
21. Miller, J.H., "*A short course in bacterial genetics: A laboratory manual and handbook for Escherichia coli and related bacteria*." 1992, Cold Spring Harbor: Cold Spring Harbor Press.
22. Walton, A.Z. and J.D. Stewart, *Understanding and improving NADPH-dependent reactions by nongrowing Escherichia coli cells.* Biotechnology Progress, 2004. **20**(2): p. 403-411.
23. Khankal, R., *STUDYING AND IMPROVING XYLOSE UPTAKE AND UTILIZATION IN ESCHERICHIA COLI*, in *Chemical Engineering*. 2009, Pennsylvania State University: University Park.
24. Eyschen, J., et al., *Engineered glycolytic glyceraldehyde-3-phosphate dehydrogenase binds the anti conformation of NAD(+) nicotinamide but does not experience A-specific hydride transfer.* Archives of Biochemistry and Biophysics, 1999. **364**(2): p. 219-227.
25. Iddar, A., et al., *Expression, purification, and characterization of recombinant nonphosphorylating NADP-dependent glyceraldehyde-3-phosphate dehydrogenase from Clostridium acetobutylicum.* Protein Expr Purif, 2002. **25**(3): p. 519-26.
26. Martinez, I., et al., *Replacing Escherichia coli NAD-dependent glyceraldehyde 3-phosphate dehydrogenase (GAPDH) with a NADP-dependent enzyme from Clostridium acetobutylicum facilitates NADPH dependent pathways.* Metab Eng, 2008. **10**(6): p. 352-9.
27. Berrios-Rivera, S.J., K.Y. San, and G.N. Bennett, *The effect of NAPRTase overexpression on the total levels of NAD, the NADH/NAD+ ratio, and the distribution of metabolites in Escherichia coli.* Metab Eng, 2002. **4**(3): p. 238-47.
28. Wubbolts, M.G., et al., *Variation of cofactor levels in Escherichia coli. Sequence analysis and expression of the pncB gene encoding nicotinic acid phosphoribosyltransferase.* J Biol Chem, 1990. **265**(29): p. 17665-72.

ACADEMIC VITA

Renae C. Patch

Rcpatch8@gmail.com

Permanent Address
219 Harris Circle
Newark, DE 19711
(302) 234-7595

Education
B.S. Chemical Engineering, Bioprocess option with Honors in Chemical Engineering
The Pennsylvania State University, University Park, PA
May 2010

Honors Thesis
Exploring the effects of overexpressing an $NADP^+$-dependent GAPDH and the NAD^+ salvage pathway on cofactor availability for NADPH-dependent biotransformation in *Escherichia coli.*
Thesis Supervisor: Dr. Patrick Cirino

Professional Experience
Army Research Lab Internship, June-August 2007
Department of Defense, Aberdeen, Maryland

- Contributed to research involving supercomputer simulations and molecular dynamics calculations of induced stress on a gold beam coated with self-assembled monolayers
- Intern under the High Performance Technologies, Inc. branch

Awards, Scholarships, and Fellowships

- Department of Chemical Engineering Bio-Fellowship, Summer 2009
- William and Wyllis Leonhard Honors Program, 2006-2010
- Schreyer Honors College Academic Excellence Scholarship, 2006-2010
- Robert P. Byrd Scholarship, 2006-2010
- College of Engineering Dean's List, Fall 2006-Spring 2008, Spring 2009-Spring 2010

Activities

- Penn State Dance MaraTHON, 2006-2010
    - Supply Logistics Captain: 2009 & 2010
    - Morale Committee member: 2008
    - Rules & Regulations Committee member: 2007
- Penn State Women's Soccer Club
    - Team Secretary & Captain: 2009
    - NIRSA National Finalists: 2009

- Penn State Athletics, 2008-2010
    - Fitness Center Desk Attendant: 2008-2010
- American Institute of Chemical Engineers (AIChE) member, 2006-2010
- Women in Engineering Program (WEP) member, 2006-2009

International Experience

- Completed 6-week Penn State Education Abroad Program in Italy, 2008
    - Completed intermediate level Italian course
    - Home-stay program